

Measurements of direct photons in Au+Au collisions with PHENIX

Benjamin Bannier (for the PHENIX collaboration)

Department of Physics and Astronomy, Stony Brook University, Stony Brook, NY 11794, USA

Abstract

The PHENIX experiment has published direct photon yields and elliptic flow coefficients v_2 from Au+Au collisions at RHIC energies [1, 2]. These results have sparked much theoretical discussion. The measured yields and flow parameters are difficult to reconcile in current model calculations of thermal radiation based on hydrodynamic time evolution of the collision volume. Our latest analyses which use high statistics data from the 2007 and 2010 runs allow the determination of direct photon yields with finer granularity in centrality and photon momentum and down to p_T as low as 0.4 GeV/c. We will summarize the current status and present new results from PHENIX.

Keywords: Direct photons

1. Introduction

Direct photons which are photons not produced in late hadron decays have been considered an excellent tool to characterize the strongly interacting states of matter produced in heavy-ion collisions for a long time. Photons are produced during all stages of the evolution of the colliding system and transport information about their production environment to the detector virtually undistorted due to their very small interaction cross section with the strongly interacting medium.

While the large yield of soft direct photons with $1 \text{ GeV}/c \lesssim p_T \lesssim 3 \text{ GeV}/c$ seen in central Au+Au collisions at RHIC [1] hints at an enhanced production of *thermal* direct photons from an early, hotter medium, the observation of strong elliptical flow v_2 of direct photons under similar conditions [2] where direct photons showed a v_2 *en par* with that of hadrons seemed an indication of very late production. Similar observations were made at LHC energies in Pb+Pb collisions [3, 4]. Accommodating both a large direct photon yield and flow has been a challenge for models. To provide further constraints on mechanisms of direct photon production PHENIX has measured the centrality-dependence of the direct photon yield and extended the p_T -coverage of the measurement to lower momenta $p_T > 0.4 \text{ GeV}/c$.

2. Method

Since measurements of soft photons in electromagnetic calorimeters are notoriously difficult due to the large hadronic backgrounds in heavy-ion collisions we reconstruct real photons from electron-positron pairs produced in external conversions of photons in the detector material [5] which allows us to take advantage of good electron reconstruction capabilities with PHENIX down to $p_T = 0.2 \text{ GeV}/c$. With this method we are able to reconstruct photons down to twice the minimal momentum for electrons, i.e. $p_T = 0.4 \text{ GeV}/c$. To minimize dependence on exact knowledge of e.g. the material budget of the detector we measure the direct photon yield indirectly via a double ratio

$$R_\gamma = \frac{Y_{\text{incl}}^\gamma}{Y_{\text{hadron}}^\gamma} = \frac{\langle \epsilon f \rangle \left(\frac{N_{\text{incl}}^\gamma}{N_{\pi^0}^\gamma} \right)_{\text{data}}}{\left(\frac{Y_{\text{hadron}}^\gamma}{Y_{\pi^0}^\gamma} \right)_{\text{sim}}} \quad (1)$$

where Y_{incl}^γ and $Y_{\text{hadron}/\pi^0}^\gamma$ denote yields of photons *produced* inclusively or in hadron/ π^0 decays, and N_{incl}^γ and $N_{\pi^0}^\gamma$ are the *observed* inclusive photon yield and the *observed* yield of photons from π^0 decays which. We directly measure the π^0 decay photon contribution to the inclusive photon yield (which represents $\sim 80\%$ of it) by tagging. The factor $\langle \epsilon f \rangle$ corrects for the finite efficiency with which photons from π^0 decays can be tagged experimentally. With this definition $R_\gamma \geq 1$ always, and $R_\gamma > 1$ is an observation of direct photons.

2.1. Inclusive photon sample N_{incl}^γ

Since the PHENIX tracking system [6] uses detectors operated 2 m or further away from the interaction vertex track reconstruction is done assuming particle tracks originating from the nominal vertex position. In this procedure momenta of particles originating from off-vertex locations $R > 0$ are misreconstructed since the actual bending angle of the particle due the magnetic field is smaller than when assuming travel through the full magnetic field. Since the PHENIX magnetic field is roughly parallel to the beam axis for measurements in the central arm detectors this leads to off-vertex particles being reconstructed with artificially larger momenta. By the same process electron-positron pairs from off-vertex conversions are reconstructed with larger and larger masses the further out radially the conversion occurred.

During the 2007 and 2010 RHIC heavy-ion runs the Hadron Blind Detector (HBD) [7] was installed before the tracking detectors whose backplane components (readout boards and chips, and electronics) at radial positions $R \approx 60$ cm provide spatially defined conversion locations with $X/X_0 \approx 3\%$. Momenta of tracks were calculated assuming production at the vertex, and assuming production from the $R \approx 60$ cm. Electron-positron pairs from conversions in the HBD backplane have fake invariant masses $m_{ee} > 0$ in the standard procedure, but are seen with $m_{ee} \approx 0$ under the off-vertex assumption. Conversely, electron-positron pairs from π^0 -Dalitz decays have correct mass $m_{ee} \approx 0$ in the standard procedure, but a fake $m_{ee} > 0$ assuming off-vertex production. By selecting on both masses we are able to extract a sample of real photons with purity $> 99\%$.

The observed yield of HBD backplane conversion pairs is related to the actual photon yield by detector- and reconstruction-dependent factors, $N_{\text{incl}}^\gamma = Y_{\text{incl}}^\gamma p_{\text{conv}} a_{ee} \epsilon_{ee}$, specifically the conversion probability in the HBD backplane p_{conv} , the geometrical acceptance for the electron-positron pair a_{ee} and reconstruction efficiency of the pair ϵ_{ee} . We measured N_{incl}^γ as a function of the converted photon p_T .

2.2. π^0 -tagged photon sample $N_{\pi^0}^\gamma$

To measure the yield of photons from π^0 decays we use an additional photon detected conventionally in the electromagnetic calorimeter which we pair with the photon reconstructed in the conversion pair. For the second photon we use very loose cuts in order to maintain maximal photon efficiency and to minimize the effect of systematic uncertainties on the final result. After modelling the combinatorial background in photon-photon pairs with a mixed event technique the observed photon yield from π^0 decays is determined by integrating mass peaks in the photon-photon mass spectrum around the π^0 mass. Since we measure the π^0 -tagged yield as a function of converted photon p_T , the converted photon introduces the identical detector- and reconstruction-specific factors as for the inclusive sample, but additionally depends on the conditional acceptance-efficiency to reconstruct the second photon from a π^0 decay in the calorimeter given we already reconstructed the first photon in a conversion pair, $\langle \epsilon f \rangle$. Specifically we have $N_{\pi^0}^\gamma = Y_{\pi^0}^\gamma p_{\text{conv}} a_{ee} \epsilon_{ee} \times \langle \epsilon f \rangle$. Now in the upper ratio in Eq. (1) the detector- and reconstruction dependent factors cancel explicitly and it only depends on the physical yields and $\langle \epsilon f \rangle$.

2.3. The tagging efficiency correction $\langle \epsilon f \rangle$

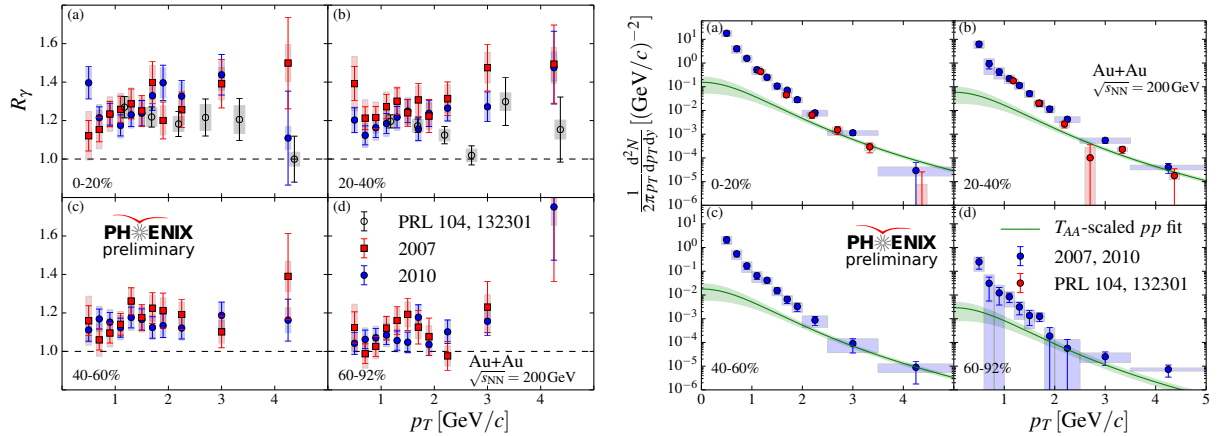
The tagging efficiency $\langle \epsilon f \rangle$ depends on the geometrical acceptance for photons measured in the calorimeter f and their reconstruction efficiency ϵ . Since we use only very loose cuts on the second photon $\epsilon \approx 90\%$, while f can be calculated accurately from the known detector geometry and knowledge of the distribution of live channels in the calorimeter. With known kinematic distributions of parent π^0 and decay kinematics the centrality-dependent factors $\langle \epsilon f \rangle$ were then calculated in a Monte Carlo simulation as functions of converted photon p_T .

2.4. The ratio $\frac{Y_{\text{hadron}}^\gamma}{Y_{\pi^0}^\gamma}$

Finally, the yield ratio between all hadron sources and exclusively from π^0 decays can be calculated in a Monte Carlo simulation independent of the detector specifics. We include the following photon production channels in our calculation: $\pi^0 \rightarrow \gamma\gamma$, $\eta \rightarrow \gamma\gamma$, $\pi^+\pi^-\gamma$, $\eta' \rightarrow \gamma\gamma$, $\pi^+\pi^-\gamma$, $\omega\gamma$, $\omega \rightarrow \pi^0\gamma$. The shapes of $\pi^0 p_T$ spectra are derived from π data [8] and derived assuming m_T scaling for the shape for other hadronic sources. The meson/ π^0 ratios are constrained by data [8, 9].

3. Results

The R_γ measured in the 2007 and 2010 data set in centrality classes 0-20%, 20-40%, 40-60% and 60-92% are shown in Fig. 1(a) where for the 2007 data set (ϵf) was determined with full Geant simulation while for the 2010 data set it was determined in a fast Monte Carlo simulation. We obtain consistent results between the two measurements, and can confirm the previous virtual photon analysis. We find that R_γ approaches unity when going to more peripheral collisions. With the additional measurements at lower momenta we find at best a weak dependence of R_γ on the photon momentum. In the following we will use run-specific corrections (ϵf) determined with the fast Monte Carlo simulation for both the 2007 and 2010 data sets. The combined 2007+2010 can be calculated from the weighted average of the data ratios (numerators in Eq. (1)) where systematic uncertainties are completely correlated. The denominators in Eq. (1) do not depend on the specific year.

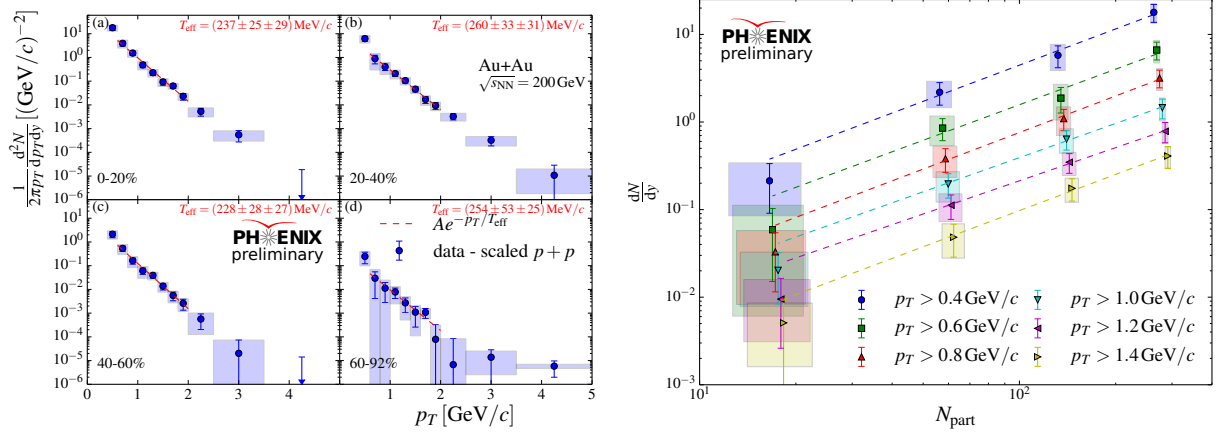


(a) R_γ measured in external conversion pairs in the 2007 and 2010 data set (filled circles and squares) and from the virtual photon analysis [1] (open circles).

(b) The direct photon p_T spectrum measured in external conversion pairs from the 2007+2010 combined data set (blue circles) and from the virtual photon analysis [1]. The green line is an N_{coll} -scaled fit to the $p+p$ data, see the text for details.

Figure 1.

With the cocktail of hadronic photon sources described in Section 2.4 we can calculate the direct photon momentum spectra shown in Fig. 1(b) from $Y_{\text{direct}}^\gamma = (R_\gamma - 1)Y_{\text{hadron}}^\gamma$ with $Y_{\text{direct,hadron}}^\gamma$ the physical yields of direct and hadron decay photons, respectively. To isolate the purely medium-induced component of the direct photon signal we parametrize the direct photon signal from prompt production measured in $p+p$ collisions [1, 10, 11] with a modified power law $a \left(1 + \frac{p_T^2}{b}\right)^{-c}$ which we scale for each centrality class according to the number of binary collisions, also shown in Fig. 1(b). After subtraction of this hard component from the scaled $p+p$ fits we arrive at the excess photon spectra shown in Fig. 2(a). The excess spectra are clearly not exponential in the shown momentum range which might be expected given the non-zero photon flow. To characterize the shape of the spectra in the low-momentum range we fit exponentials $Ae^{-p_T/T_{\text{eff}}}$ in the range $0.6 \text{ GeV/c} < p_T < 2.0 \text{ GeV/c}$ where the inverse slope parameter T_{eff} should be interpreted exclusively as a shape parameter for this discussion since due to direct photon flow extractions of the medium temperature from the spectra are not obvious [12]. We find remarkably similar values for the inverse slope



(a) The excess photon spectra in external conversion pairs from the 2007+2010 combined data set. The dashed lines are exponential fits in the range $0.6 \text{ GeV}/c < p_T < 2.0 \text{ GeV}/c$

(b) The integrated excess photon yield as a function of N_{part} for different lower integration limits. The dashed lines are independent fits AN_{part}^x to each set of points.

Figure 2.

across centralities within the given uncertainties while the yield varies over more than 2 orders of magnitude. The inverse slopes extracted here are overall compatible with the earlier PHENIX measurement from virtual photons [1] which were extracted in a slightly higher momentum range. We find that the direct photon spectra at RHIC energies are softer than at LHC where ALICE has extracted $T_{\text{LHC}} = (304 \pm 51^{\text{syst+stat}}) \text{ MeV}$ [3].

To characterize the centrality-dependence of the excess photon spectra we calculate integrated yields,

$$\frac{dN}{dy} = 2\pi \int_{p_{T,\text{min}}}^{5 \text{ GeV}/c} dp_T p_T \left(\frac{1}{2\pi p_T} \frac{d^2N}{dp_T dy} \right).$$

Since the excess photon spectra are steeply falling functions of photon p_T the integrated yields will depend mostly on the lowest few measurements in the spectra. To not prefer one momentum range over another we calculate integrated yields for all possible lower integration limits in the range $0.4 \text{ GeV}/c < p_T < 1.4 \text{ GeV}/c$ while leaving the upper limit fixed at the end of our measured range. In Fig. 2(b) we show the integrated yields as a function of Glauber N_{part} . We find a power law dependence with power $1.48 \pm 0.08(\text{stat}) \pm 0.04(\text{syst})$ of the integrated yield on N_{part} , independent of the considered p_T -range reflecting the similar inverse slopes observed earlier. The yield of hadrons grows roughly linear with N_{part} .

References

- [1] A. Adare, et al., Enhanced production of direct photons in Au+Au collisions at $\sqrt{s_{NN}} = 200 \text{ GeV}$ and implications for the initial temperature, Phys.Rev.Lett. 104 (2010) 132301.
- [2] A. Adare, et al., Observation of direct-photon collective flow in $\sqrt{s_{NN}} = 200 \text{ GeV}$ Au+Au collisions, Phys.Rev.Lett. 109 (2012) 122302.
- [3] M. Wilde, Measurement of Direct Photons in pp and Pb-Pb Collisions with ALICE, Nucl.Phys. A904-905 (2013) 573c–576c.
- [4] D. Lohner, Measurement of Direct-Photon Elliptic Flow in Pb-Pb Collisions at $\sqrt{s_{NN}} = 2.76 \text{ TeV}$, J.Phys.Conf.Ser. 446 (2013) 012028.
- [5] R. Petti, Direct photons in Au+Au collisions measured with the PHENIX detector at RHIC, J.Phys.Conf.Ser. 316 (2011) 012026.
- [6] K. Adcox, et al., PHENIX central arm tracking detectors, Nucl.Instrum.Meth. A499 (2003) 489–507.
- [7] W. Anderson, B. Azmoun, A. Cherlin, C. Chi, Z. Citron, et al., Design, Construction, Operation and Performance of a Hadron Blind Detector for the PHENIX Experiment, Nucl.Instrum.Meth. A646 (2011) 35–58. arXiv:1103.4277.
- [8] A. Adare, et al., Detailed measurement of the e^+e^- pair continuum in $p+p$ and Au+Au collisions at $\sqrt{s_{NN}} = 200 \text{ GeV}$ and implications for direct photon production, Phys.Rev. C81 (2010) 034911. doi:10.1103/PhysRevC.81.034911.
- [9] A. Adare, et al., Neutral pion production with respect to centrality and reaction plane in Au+Au collisions at $\sqrt{s_{NN}}=200 \text{ GeV}$, Phys.Rev. C87 (2013) 034911.
- [10] S. Adler, et al., Measurement of direct photon production in $p+p$ collisions at $\sqrt{s} = 200 \text{ GeV}$, Phys.Rev.Lett. 98 (2007) 012002.
- [11] A. Adare, et al., Direct-Photon Production in $p+p$ Collisions at $\sqrt{s} = 200 \text{ GeV}$ at Midrapidity, Phys.Rev. D86 (2012) 072008.
- [12] C. Shen, U. W. Heinz, J.-F. Paquet, C. Gale, Thermal photons as a quark-gluon plasma thermometer revisited arXiv:1308.2440.